Evolution of domain structures in Na_{1/2}Bi_{1/2}TiO_{3} single crystals with BaTiO_{3}

Jianjun Yao, Li Yan, Wenwei Ge, Liang Luo, Jiefang Li, D. Viehland, Qinhui Zhang, and Haosu Luo

Evolution of domain structures in $Na_{1/2}Bi_{1/2}TiO_3$ single crystals with $BaTiO_3$

Jianjun Yao*, Li Yan, Wenwei Ge, Liang Luo, Jiefang Li, and D.Viehland

Department of Materials Science and Engineering, Virginia Tech, Blacksburg, Virginia 24061

Qinhui Zhang and Haosu Luo

Shanghai Institute of Ceramics, Chinese Academy of Sciences, 215 Chengbei Road, Jiading, Shanghai 201800, China

The domain structures of $Na_{1/2}Bi_{1/2}TiO_3$-Ba_xTiO_3 (NBT-x%BT) crystals for x=0, 4.5 and 5.5% have been investigated by polarized light and piezoresponse force microscopies. The results show that $BaTiO_3$ (i) refines the size of polar nano-regions and enhances their self-organization; and (ii) suppresses formation of proper ferroelastic domains at high temperatures in the paraelectric state, and rather favors the formation of improper ones that form below the ferroelectric Curie temperature that elastically accommodate the ferroelectric ones.

*Email: jjyao@vt.edu

I. Introduction

Lead-free $Na_{1/2}Bi_{1/2}TiO_3$ (NBT) piezoelectrics have received much attention due to environmental concerns.[1-4] Structural investigations by X-ray (XRD) and neutron diffractions have revealed a morphotropic phase boundary (MPB) in the NBT-x%BaTiO$_3$ (NBT-x%BT) solid solution for 6<x<7, where piezoelectric coefficients as high as 480 pC/N have recently been reported.[5] It is known that NBT undergoes a phase transformational sequence of paraelectric cubic (C) →paraelectric tetragonal (T) →ferroelectric rhombohedral (R) on cooling [6-10]: with transition temperatures of about 550 and 300□, respectively.

Investigations of the domain structure of NBT and NBT-x%BT have previously been performed by transmission electron microscopy (TEM). [11,12] Domains were not observed by TEM for x=3 and 8 [12]: which might be due to electron beam effects.[13] However, polarized light microscopy (PLM) studies of NBT (i.e., x=0) have shown the presence of ferroelastic domains of size 10-100μm in the high temperature paraelectric T phase [14]. These ferroelastic domains form on cooling at the T→C phase boundary near 550□. Clearly, the T domains must be proper ferroelastics. Proper ferroelastic twins form to achieve elastic compatibility between regions of different orientational variants having strain as a spontaneous order parameter [15]. Improper ferroelastic twins can accompany ferroelectric domain formation, due to an electrostrictive coupling of the polarization to the lattice strain [16]. But, improper ferroelastic twins disappear on heating above the ferroelectric→paraelectric boundary.

Scanning probe microscopy (SPM), performed in the piezoresponse mode (PFM), provides a way to study the ferroelectric domain structures at various length scales with high spatial resolution [17], and could be used to study the ferroelectric domains of NBT-x%BT. In fact,

recent investigations of NBT by PFM have revealed the presence of polar nano-regions in the ferroelectric R phase field [14]. Formation of these nano-regions occurs on cooling at temperatures below the dielectric maximum (T_m). Interestingly, the high temperature ferroelastic T domains remained present in the ferroelectric R phase field, as shown by PLM.

Here, we report an investigation of the evolution of the domain structure of (001) oriented crystals of NBT-x%BT for x=0, 4.5, and 5.5 by means of PFM and PLM. Investigations were focused on revealing how the domain structure changes with the addition of BT, as the MPB is approached. The results show with increasing x that (i) the polar nano-region width is decreased, and the nano-regions become increasingly self-organized; and (ii) the formation of proper tetragonal ferroelastic domains is suppressed, and rather improper ferroelastic ones formed below the ferroelectric Curie temperature. Our findings provide insights into why the piezoelectric properties of NBT-x%BT are enhanced with increasing x, as the MPB is approached.

II. Experimental Procedure

Single crystals of NBT, NBT-4.5%BT and NBT-5.5%BT were grown by a top-seeded solution growth (TSSG) method [18]. <001> oriented wafers of NBT, NBT-4.5%BT and NBT-5.5%BT single crystals were cut into dimensions of $3\times3\times0.3mm^3$, and the surfaces were polished down to 0.3 μm finishes. Careful investigations of the domain structure were performed by scanning probe microscopy using the piezo-force mode (DI 3100a, Veeco); and by polarized light microscopy (PLM) using a Leica Microsystem (Wetzlar Gmbh) equipped with a crossed polarizer–analyzer (P/A) pair and a Linkam THMS600 (Linkam Scientific Instruments Ltd.,Tadworth, Surrey, U.K.) temperature control stage. Before measurements, all crystals were annealed at 900 K for 30 min. Careful investigations were performed starting from the annealed

condition. Gold electrodes were deposited on the bottom face of each sample by sputtering. During PFM studies, the electrode faces were then glued to the sample stage, and the opposite unelectroded surface was scanned by the SPM tip. All scans were performed at room temperature, using a conductive silicon tip coated with cobalt. An ac modulation voltage of 5V (peak to peak) with a frequency of 20 kHz was applied between the conductive tip and the bottom gold electrode.

III. Results.

1. *Room temperature studies of polar domain structures for various x% by PFM.*

Figure 1 shows PFM images of unpoled (001)-oriented crystals for (a) x=0, (b) 4.5% and (c) 5.5%. The image for NBT reveals the presence of polar nano-regions (PNRs) that are on the order of 50nm to 500nm in size, as recently reported [14]. It is worth to note that the PNRs for NBT can be expected to have a size of about 10nm,[19] and in fact, recently published TEM images are consistent with this expectation.[20] However, for NBT, the size of the PNRs revealed by PFM is considerably larger, and no self-organization into periodic patterns was found. It is possible that individual PNR are not able to be observed by PFM due to a small value of d_{33} that provides modest contrast: rather we may only observe colonies of them that are not well-organized. These nano-regions may not have appeared well organized, although optical diffractograms obtained by fast Fourier transforms showed some tendency to organize along the <110>. Furthermore, their distribution was not very uniform, and the boundaries between regions were quite rough.

With increasing BaTiO$_3$ content to 4.5%, the distribution of nano-regions became more uniform than for NBT. In particular, the length became notably longer along the <110> with sizes

on average of >1µm. Furthermore, the boundaries between regions became much smoother. The labyrinthine domain pattern is indicative of the local deviation of surface symmetry from cubic [20]. With further increasing BT to 5.5%, these changes became more pronounced: with lengths becoming on average >2 µm. One notable difference with increasing BT content between x=4.5% to 5.5% was that the widths of the polar regions were refined to a thickness of <100nm. As the MPB region was approached, this increased length and decreased width resulted in a stripe-like morphology with an orientation along the <110>. These results clearly show a tendency of increased self-organization of the polar regions with increasing BT. Polar nano-regions organized into stripe-like domains of increasing length along the <110>. These changes with x%BT are similar to those previously reported for $Pb(Mg_{1/3}Nb_{2/3})O3-x\%PbTiO_3$ (PMN-x%PT) with increasing x%PT [22,23] as the MPB region in that solution was also approached.

2. *Temperature dependent studies for various x% by PLM.*

Polarized light microscopy is widely used in transmission geometry and the principle of setup in our case is as following: the orientation herein is based on the axis of a prototype cubic phase of the perovskite structure. Based on the lattice symmetry, when a single crystal sample is observed along the crystallographic <001> direction under cross-polarized light, domains of the T phase exhibit optical extinctions when the polarizer is set along the <100> or <010> directions. For domains of the R phase, they exhibit optical extinction when the polarizer is set along the <110> crystallographic directions, namely in an angle of 45^0 with respect to the [010] direction. This enables us to distinguish the possible different phases in the crystals.

Figure 2 shows the PLM images of (001)-oriented NBT taken at temperatures of (a) 25□, and (b) 550□. Comparisons of these figures will reveal that structural domains oriented along the <110> formed on cooling below 550□, as recently reported [14]. The domain lengths were on the order of hundreds of microns, and their widths between 5 and 100μm. Please note that we used reflected light to observe domain formation, and that the results are consistent with those obtained using polarized light where optical extinction was found to occur at 550□ in the C phase field. The formation of these domains corresponded in temperature to that of the paraelectric C→paraelectric T phase boundary [14], which is far above that of the dielectric maximum at about T_m=330□. The crystal lattice parameters of this phase were confirmed by x-ray diffraction to be tetragonal with c/a≈1.01. Clearly, these tetragonal structural domains are proper ferroelastic ones.

Interestingly, these T ferroelastic domains persisted on cooling into the ferroelectric R phase field below 300□, and remained nearly unchanged at 25□. This demonstrates that the invariant conditions established to relax the elastic energy in the T phase persist into the R phase field, even though the structure is no longer tetragonally distorted and that c/a≈1.00: i.e., there is a geometrical and elastic inheritance from the parent paraelectric/ferroelastic tetragonal phase into the product ferroelectric rhombohedral one. On cooling below the T→R phase boundary, polar nano-regions formed, as discussed above with reference to Fig.1c (25□), and as re-shown in Fig.2c at higher resolution for comparative purpose with the PLM images.

These findings for NBT thus demonstrate the presence of two different types of co-existing domains in NBT: large (10-100μm) proper ferroelastic ones that form at high temperatures, and much smaller (100-500nm) polar regions that form at lower temperatures. The polar regions are

embedded in the T ferroelastic domains. Please note that the ferroelastic domain structure does not form or change to stress-accommodate the polar ones. The polar R regions do not assemble into bands defined by the invariant plane strain to relax stress [24], but rather nucleate within the pre-existing geometrical restrictions of the proper ferroelastic domains.

Figure 3 shows the PLM images for NBT-4.5%BT at temperatures of (a) 25□, and (b) 176□. At room temperature, macrodomain platelets notably larger than those for NBT were observed: which were of length >500μm and of width ≈50μm. These domain platelets for NBT-4.5%BT were oriented along the <100> direction, rather than the <110> as for NBT. We note that the domain platelets were observed when one of the P/A axes was oriented along the $<100>_{cub}$ and when the polarizer was set along the <110> directions that optical extinction was found. This infers that no true T ferroelastic phase exists in NBT-4.5%BT as for NBT, and that these macrodomain platelets have the Rhombohedral structure. Furthermore, these macrodomain platelets for NBT-4.5%BT were found to disappear on heating above 175□, as can be seen in Fig.3b. This temperature was notably below that of the dielectric maximum of T_m=300□, and rather is close to that previously attributed to a transformation between ferroelectric and antiferroelectric R phases [25]. Clearly, significant and important changes have occurred with regards to the nature of these macrodomain platelets with increasing BT content. It is important to note that structural studies by XRD failed to reveal a tetragonal phase at temperatures above the dielectric maximum for x>2 (data not shown); rather, the phase transformational sequence on cooling was found to be paraelectric C→R. Comparisons of these data with our finding demonstrate that the platelets for NBT-4.5%BT are not true tetragonal ferroelastic domains.

Furthermore, these changes in macrodomain platelets with x% were accompanied by important changes in the self-organization of the polar regions as observed by PFM, and as re-shown in Fig.3c at higher resolution for comparative purpose; where stripe-like domains were found that were of width 150nm and of lengths >1μm. Please note that self-organization occurs along the <110>, which is the direction along which elastic compatibility can be achieved for either R or T domains. These results strongly indicate an important role of stress accommodation between polar nano-regions in the self-organization process.

Similar results can be seen in the PLM images given in Figure 4 for NBT-5.5%BT at temperatures of (a) 25□, and (b) 155□. Again, macrodomain platelets can be seen that are oriented along the <100>, although they are notably larger than those than those for NBT-4.5%BT. In particular, the widths were increased to about 200-400μm, as the MPB compositional region was approached. These macrodomain platelets disappeared on heating at 155□, which was notably below the dielectric maximum at 300□. A PFM image at high resolution is re-shown in Fig.4c for comparative purposes, which reveals similar features as those for NBT-4.5%BT: with the exception that the polar regions were longer and narrower, as noted above.

These findings for NBT-4.5%BT and NBT-5.5%BT thus demonstrate the presence of a ferroelectric domain structure, which minimizes its elastic energy by the geometrical arrangement of ferroelectric domains into macrodomain platelets. Such types of stress-accommodating domain structures are typical of any displacive transformation, which can achieve a domain-averaged transformation strain that is an invariant plane strain [24]. These macrodomain platelets for NBT-4.5%BT and NBT-5.5%BT are not true ferroelastic domains, but rather are improper

ferroelastic ones that arise due to the electrostrictive coupling of the spontaneous polarization to the lattice.

IV. Discussion and Summary.

Clearly, there are dramatic changes in the domain structure(s) of NBT-x%BT with modest changes in x, as the MPB is approached. Before we turn to the analysis of the domain structure of NBT-x%BT, here we are going to discuss a couple of possible factors existed in experiments which would help in understanding the data better.

First, consideration of surface state and specimen choosing, surface states or "skin effects" are known in PMN-x%PT relaxors.[21,26,27] These surface states result in an apparent "phase X" or distorted Cubic. However such surface states have not been reported to have either Rhombohedral or Tetragonal structures. Studies of PMN-x%PT by PFM have revealed PNRs for composition of x<30at.%, where "phase X" and a Cubic phase (x<25at.%) are known.[23] Such surface states in PMN-x%PT do not exhibit self-organization of PNRs into somewhat periodic arrangements until when the Monoclinic and Tetragonal phases are stable near the MPB. In this region of the PMN-x%PT phase diagram (i.e., where Mc and T phases are stable), surface states are not found.

The possibility that the PNRs of NBT might have influence from the surface condition was considered. Recent TEM images [20] reveal PNRs that are similar in morphology to those by PFM: however, those by PFM are larger. We are not for sure if it is a surface effect that makes them appear larger, or rather the low d_{33} of 25 pC/N reduces the contrast in the PFM image. Probably, colonies of PNRs in NBT were imaged whose individual PNRs cannot be resolved because of a low d_{33}. It is noted that the self-organization of PNRs into more periodic twin

structures with increasing x at.%BT is much like that of PMN-x%PT near its MPB.[23] However, surface states are not the cause, rather relaxation of the elastic energy by stress accommodation.

In order to verify that our observations on the ferroelectric domains have validity to the bulk, two issues need to be mentioned. First, elastic accommodation that drives self-assembly of the polar nano-regions into more periodic arrays is a long-range force. It achieves a lower energy configuration by volume effects. Such changes in domains with xat.% have validity not just to surface states, but rather to bulk ones. Second, charge compensation during the PFM imaging needs to be considered. In this study, the effect of small AC biases applied to the PFM tip and to the bottom of the sample was compared: both cases showed similar results. If charge compensation occurred, the results of the two cases would not be the same. Therefore, it can be inferred that the effect of charge compensation on PFM images is negligible for the NBT-x%BT system. In order to minimize the possible influence of a charged PFM tip on the surface domains, especially for electrostatic tip-surface interactions, the PFM tip (DDESP, Veeco) with a cantilever spring constant of 20-80N/m was used, which should guarantee that the influence of a charged PFM tip on domains is negligible in present study.[28-30]

Next we attempt to summarize the changes we observed in section III into a diagram, as shown in Figure 5. Please note that we begin by using the previously published NBT-x%BT phase diagram [1], and superimpose on this diagram changes in domain stability. We refrain here forward from referring to it as the equilibrium phase diagram.

First, we modified the diagram by including at low BT concentrations of x<2% the high temperature tetragonal paraelectric phase. The C$\rightarrow$T phase boundary for NBT is shown to be at

about 550□, and is represented by a solid point. However, we do not know for sure what happens to the C→T phase boundary with small increases in x, other than the simple fact that it disappears by x≈2%. This was confirmed both by recent XRD studies which reveal that the c/a splitting of the T phase disappears (data not shown), and the fact that we observe the T ferroelastic domains to disappear for x<4%. Thus, we represent the C→paraelectric T phase boundary for x<2% by a dashed line. In this paraelectric T phase field, we show that true ferroelastic domains are present. These ferroelastic domains are of length >100μm and were oriented along the <110> direction.

An intermediate phase field is shown that is sandwiched between the paraelectric and ferroelectric phases. We refrain from assigning the crystal class for this phase field. Prior investigations have given evidence of intermediate antiferroelectric phases that are rhombohedral [2], structurally modulated orthorhombic phases [31], and tetragonal ferroelectric phases [32]. Our recent investigations by PLM [14] have shown that on cooling between 320 and 200℃ that there are gradual changes in the optical extinction conditions, indicating a diffuse transformation region, where R polar regions gradually nucleate and increase in volume fraction with decreasing temperature. This is consistent with the broad dielectric constant maximum, which is also a hallmark feature of a diffuse transformation [33]. Our recent XRD studies showed that the average structure in this temperature range is pseudo-cubic. However, we note that within this pseudo-cubic structure that polar nano-regions that are electrostrictive exists, which are elastically clamped by their matrix. Thus, it is possible that alternative near-degenerate thermodynamically metastable states could exist, that try to relax the elastic energy of clamped elastically distorted polar nano-regions: which might rationalize the various differing results from prior studies. We designate this phase field in the diagram as a diffuse phase transformation

region, where R polar regions nucleate that are elastically clamped. The upper boundary between this phase field and the paraelectric state is defined by the temperature of the dielectric maximum [34-37]. The lower boundary between this phase field and the rhombohedral ferroelectric state is defined by the onset of frequency dispersion in the dielectric constant [34-37]. We note that both of these boundaries, although previously shown in published phase diagrams defining an antiferroelectric phase, are imprecise: thus, we also denote them as dashed lines.

Next, we show the low temperature rhombohedral R field for x<6%, whose upper boundary was designated just above to be determined by the onset of frequency dispersion in the dielectric constant [34-37]. We show this R phase field to be "divided" by a dashed boundary representing an unknown limit of stability for the tetragonal ferroelastic domains. For x<2%, we show in the diagram that polar R domains (which nucleate in the diffuse phase transformation region) are embedded in the T ferroelastic domains. In this area of the diagram, the entire matrix is converted into R polar nano-regions, but yet the ferroelastic domains persist. These polar nano-regions cannot stress-accommodate each other by geometrically arranging themselves into domain platelets that achieve a domain-averaged transformation strain that is an invariant plane strain. The crystal lattice parameters in this area of the diagram have been shown to be rhombohedral , with a small rhombohedral distortion angle of α_r=89.90°. For x>2%, we show in the diagram that polar R domains exists that are stess-accommodating into macrodomain platelets. These macrodomain platelets are improper ferroelastics. The crystal parameters in this area of the diagram have been shown to be (a_r,α_r)=(3.96Å, 89.98°). Thus, the average structure is nearly, if not, pseudo-cubic: similar to that of relaxor ferroeletrics.

Furthermore, in this diagram, we show the MPB region between rhombohedral and tetragonal ferroelectric phases, near x=6%. We have drawn the boundary to be wide between 5.5<x<6.5%. This is because recent investigations [38] have shown that the location of this boundary in composition space, x, can somewhat depend on the electrical history of the sample. It is interesting to note that near this MPB boundary is where the dielectric and piezoelectric constants have been reported to be maximum. The refinement of stress-accommodating ferroelectric domains may be an important contributing factor to the enhancement of the piezoelectric properties near the MPB. Refinement of ferroelectric domains would lead to an increased domain wall density, which may act as natural nucleation sites for inducing phase transitions [39]. At lower BT contents, the piezoelectric properties may be suppressed by the ferroelastic domains, which are independent of the ferroelectric ones and which seem to suppress their ability to stress-accommodate.

Finally, we try to understand the competing order parameters and we applied the Tagantsev-Balashova model [40,41] to analyze the competition of structural and ferroelectric instabilities in NBT-xat.%BT. The existence of true ferroelastic domains in the NBT-xat.%BT system makes the sequence of phase transformations more complex than the model. The most relevant equation for our use is:

$$T_c = (T_{cp} - \Delta T_{c\eta})/(1 - \Delta)$$

$$b/a = 1 - \varphi\Delta$$

where $\boldsymbol{\Delta}$ is the difference in the temperature dependence between the energies of the nonpolar ordered state and the polar state; $\boldsymbol{\varphi}$ is the coupling between these order parameters; a and b are the slopes of the reciprocal dielectric constants with temperature in the paraelectric and nonpolar ordered states, respectively. Figure 6 (a) shows the dielectric constant for NBT taken at a frequency of 100KHz: from which the structural (i.e., antiferroelectric) phase transition temperature can be seen to be $T_{c\eta}$=598K. We identified from in the dielectric data, that T_c=498Km, which corresponds to the ferroelectric phase transition temperature. The value of T_{cp}=518K was determined by the reciprocal dielectric constant extrapolated using the Curie-Weiss relationship, as shown in Figure 6(b).

We can then estimate that $\boldsymbol{\varphi}$=10.2 and $\boldsymbol{\Delta}$=0.2 for NBT. Accordingly, following the Tagantsev-Balashova model, we can ascribe the behavior to the S region, which is considered as an intermediate region between antiferroelectric and ferroelectric behaviors. This in term reveals that transformational sequence is antiferroelectric to noncritical first-order ferroelectric, the latter being accompanied by a weak dielectric anomaly.

In the S region, two conditions for independent parameters should be valid: these are $\boldsymbol{\varphi}\boldsymbol{\Delta}$>1 and $\boldsymbol{\Delta}$ <1. The first condition means that the structural order parameter, which appears at T< $T_{c\eta}$, suppresses completely the ferroelectric instability: i.e., a critical ferroelectric phase transition is impossible, as in the temperature range below $T_{c\eta}$ there is no point where the nonpolar ordered state loses its stability. The second condition ($\boldsymbol{\Delta}$<1) means that the energy of the polar state changes with temperature faster than that of the nonpolar ordered one. The temperature dependent free energies of the states are illustrated in Figure 6(c). At T_c , these conditions mean

that the energies of the two states are equal; where for T< T_c , the polar phase appears by means of a noncritical first-order ferroelectric phase transition. [40,41]

Following this approach, a structural instability is realized before the ferroelectric one at a temperature of $T_{c\eta} > T_{cp}$, and the polar state then appears by means of a non critical first-order phase transition at T_c . This transition is a result of a difference in the temperature dependence of the energies of the polar and nonpolar ordered states as illustrated in Figure 6(c). Following the Tagantsev-Balashova model, the system would enter into a paraelectric state above $T_{c\eta}$ and structural stability would be achieved.(follow the red dashed line in Fig. 6.) However for NBT, there are some important differences that we need to note, with respect to this model. As we know, NBT has an additional transition from a tetragonal paraelectric phase to a cubic paraelectric phase near 550°C. We can designate this temperature as $T'_{c\eta}$: please note that its structural instability is different in nature than that of the Tagantsev-Balashova theory. At $T_{c\eta}$, structural stability of NBT is not achieved, and the system remains unstable until the temperature $T'_{c\eta}$ is reached (as shown the revised line in Fig.6(c)).

In summary, our study shows that the addition of BaTiO$_3$ to NBT (i) refines the size of polar nano-regions and enhances their self-organization; and (ii) suppresses formation of proper ferroelastic domains at high temperatures in the paraelectric state, and rather favors the formation of improper ones that form below the ferroelectric Curie temperature that elastically accommodate the ferroelectric ones.

Reference

1. T. Takenaka, K. Maruyama and K. Sakata, Jpn. J. Appl. Phys. **30**, 2236 (1991).

2. Y. M. Chiang, G. W. Farrey and A. N. Soukhojak, Appl. Phys. Lett. **73**, 3683 (1998).

3. B. J. Chu, D. R. Chen, G. R. Li and Q. R. Yin, J. Eur. Ceram. Soc. **22**, 2115 (2002).

4. G. Smolenskii, V. Isupov, A. Agranovskaya, and N. Kainik, Sov. Phy. Solid State 2, 2651 (1961).

5. Q. Zhang, Y. Zhang, F. Wang, Y. Wang, D. Lin, X. Zhao, H. Luo, W. Ge, and D. Viehland, Appl. Phys. Lett. 95, 102904 (2009).

6. J. Zvirdzds, P. Kapostins, J. Zvirgzde, and T. Kruzina, Ferroelectrics 40, 75 (1982).

7. S. Vakhrushev, V. Isupov, B. Kvyathkovsky, N. Okeuneva, I. Pronin, G. Smolensky, P. Syrnikov, Ferroelectrics 63, 153 (1985).

8. J. Suchanicz and J. Kwapulinski, Ferroelectrics 165, 249 (1995).

9. J. Kusz, J. Suchanicz, H. Bohm, J. Warczewski, Phase Trans. 70, 223 (1999).

10. G. Jones and P. Thomas, Acta Crystallogr. B58, 168 (2002).

11. V. Dorcet, G. Trolliard, Acta. Mater. 56, 1753 (2008)

12. A.N.Soukhojak, H.Wang, G.W.Farrey, and Y.-M.Chiang, J.Phys.Chems.Solids. 61, 301 (2000)

13. Z. Xu, M.-C. Kim, J.-F. Li, and D. Viehland, Philos. Mag. A 74, 395 (1996).

14. J.J. Yao, W.W. Ge, L. Luo, J.F. Li, D. Viehland, and H.S. Luo, Appl. Phys. Lett. 96, 222905 (2010).

15. E. Salje, Ferroelectrics, 104, 111 (1990).

16. W.Cao and G.R. Barsch, Phys. Rev. B 41, 4334 (1990).

17. N. Balke, I. Bdikin, S.V., Kalinin, and A.L. Kholkin, J. Am. Ceram. Soc. 92, 1629 (2009)

18. W.W. Ge , H. Liu, X.Y. Zhao, B.J. Fang, X.B. Li, F.F. Wang, D. Zhou, P.Yu, X.M. Pan, D. Lin, and H.S. Luo, J. Phys. D-App. Phys, 41, 115403 (2008)

19. I.-K. Jeong, T. W. Darling, J. K. Lee, T. Proffen, R. H. Heffner, J. S. Park, K. S. Hong, W. Dmowski, and T. Egami, Phys. Rev.Lett. 94, 147602 (2005).

20. J.J. Yao, W.W. Ge, Y.D. Yang, L. Luo, J.F. Li, D. Viehland, S. Bhattacharyya, Q.H. Zhang, and H.S. Luo, J. Appl. Phys. 108, 064114 (2010).

21. S. V. Kalinin, B. J. Rodriguez, J. D. Budai, S. Jesse, A. N. Morozovska, A. A. Bokov and Z.-G. Ye, Phys. Rev. B 81, 064107 (2010)

22. D. Viehland, M.-C. Kim, Z. Xu, and J.-F. Li, Appl. Phys. Lett. 67, 2471 (1995)

23. F. Bai, J.F. Li, and D. Viehland, Appl. Phys. Lett. 85, 2313 (2004).

24. Y. Wang, X.B. Ren, and K.Otsuka, Phys. Rev. Lett. 97, 225703 (2006).

25. V.A. Isupov, Ferroelectrics 315, 123 (2005).

26. G.Y. Xu, Z. Zhong, Y. Bing, Z.G. Ye, C. Stock, G. Shirane, Phys. Rev. B 70, 064107 (2004)

27. G. Y. Xu, P.M. Gehring, C. Stock, K. Conlon, Phase Transitions 79, 135 (2006)

28. S.Hong, J. Woo, H. Shin, J. Jeon, Y. E. Pak, E. L. Colla, N. Setter, E.Kim, and K. No. J. Appl. Phys. 89,1377 (2001)

29. S.V. Kalinin and D. A. Bonnell. Phys. Rev. B 65, 125408 (2002)

30. F. Johann, Á. Hoffmann, and E. Soergel, Phys. Rev. B 81, 094109 (2010).

31. V. Dorcet, G. Trolliard, P. Boullay, Chem. Mater. 20, 5061 (2008).

32. S. Said, J.P. Mercurio, J. Eur. Ceram. Soc. 21, 1333 (2001).

33. C.-S.Tu, I.G. Siny, and V.H Schmidt, Phy. Rev. B 49, 11550 (1994).

34. Y. Hiruma, Y. Watanabe, H. Nagata, and T. Takenaka, Key Eng.Mater. 350, 93 (2007).

35. W. Ge, H. Liu, X. Zhao, X. Pan, T. He, D. Lin, H. Xu, and H. Luo, J. Alloys Compd. 456, 503 (2008).

36. W. W. Ge, H. Liu, X. Y. Zhao, B. J. Fang, X. B. Li, F. F. Wang, D. Zhou, P. Yu, X. M. Pan, D. Lin, and H. S. Luo, J. Phys. D: Appl. Phys. 41,115403 (2008).

37. W. W. Ge, H. Liu, X. Y. Zhao, X. B. Li, X. M. Pan, D. Lin, X.H. Xu, B. J. Fang, and H. S. Luo, Appl. Phys. A 95, 761 (2009).

38. W.W. Ge, H. Cao, J.F. Li, D. Viehland, Q.H. Zhang, and H.S. Luo, Appl. Phys. Lett. 95, 162903 (2009).

39. W. W. Cao and C. A. Randall, J. Phys. Chem. Solids 57, 1499 (1996).

40. E.V. Balashova and A.K. Tagantsev, Phys. Rev. B 48, 9979 (1993)

41. E.V. Balashova,V.V. Lemanov, A.K. Tagantsev, A.B. Sherman, and Sh.H. Shomuradov, Phys. Rev. B 51, 8747 (1995)

List of Figures

NBT

1μm

[100]

[001] [010]

NBT-4.5%BT

1μm

NBT-5.5%BT

1μm

Figure 1

Figure 1   BU11556   27DEC10

Figure 2

Figure 2   BU11556   27DEC10

a 25℃

[100]

[010]

[001]

400μm

b 176°C

400μm

c

400nm

Figure 3

Figure 3   BU11556   27DEC10

a 25°C
400μm

b 155°C
400μm

[100]
[010]
[001]

c
400nm

Figure 4

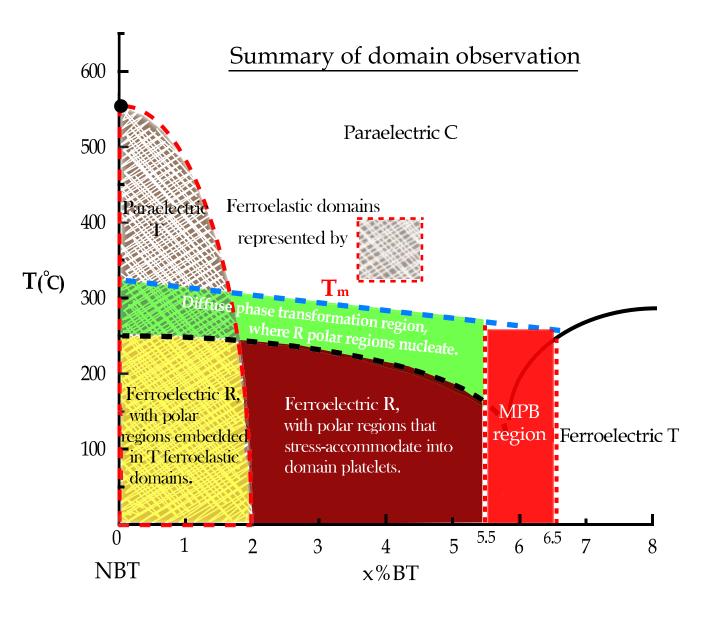Figure 4   BU11556   27DEC10

Figure 5

Figure 5   BU11556   27DEC10

Figure 6   BUIT556   27DEC10